ELSEVIER

Composites Science and Technology 62 (2002) 1151–1160

COMPOSITES SCIENCE AND TECHNOLOGY

www.elsevier.com/locate/compscitech

Delamination monitoring of graphite/epoxy laminated composite plate of electric resistance change method

Akira Todoroki*, Yuuki Tanaka, Yoshinobu Shimamura

Department of Mechanical Sciences and Engineering, Tokyo Institute of Technology, 2-12-1, Ohokayama, Meguro, Tokyo 1528552, Japan

Received 10 August 2001; received in revised form 13 February 2002; accepted 20 February 2002

Abstract

The present paper employs the electric resistance change method for monitoring of location and size of a delamination crack of graphite/epoxy composite laminates. The method is applied to a plate-type specimen with an embedded delamination of cross-ply and quasi-isotropic laminates. Ten electrodes made from copper foil are mounted on the specimen top surfaces. An embedded delamination crack is created by a static indentation test, and the electric resistance changes are measured using a conventional strain gage amplifier. Response surfaces are adopted as a tool for solving inverse problems to estimate location and size of delamination crack from the measured electric resistance changes of all segments between electrodes. As a result, the present method successfully provides estimations of location and size of the embedded delamination for graphite/epoxy laminated composites.

Keywords: C. Delamination; Electric resistance

1. Introduction

Laminated composites usually have low delamination resistance, and that causes delaminations by slight impacts. Since the delaminations are invisible or difficult to detect by visual inspections, the delamination causes low reliability for primary structures. In order to improve the low reliability, automatic systems of delamination identifications in-service are desired. A structural health monitoring system to detect the delaminations is one of the desired approaches for practical laminated composite structures.

Recently, an electric resistance change method is employed to identify the internal damages of CFRP (Carbon Fiber Reinforced Plastics) laminates by many researchers [1–18]. The electric resistance change method does not require expensive instruments. Since the method adopts reinforcement carbon fiber itself as sensors for damage detections, this method does not cause reduction of static strength or fatigue strength, and it is applicable to existing structures.

Authors have already experimentally investigated the applicability of the electric resistance change method for measurements of delamination crack length of the edge cracks of delamination resistance tests [19,20]. For practical composite structures, however, delamination cracks are usually embedded cracks. The embedded cracks of the beam type specimens were also experimentally detected by the electric resistance change method by Todoroki using graphite/PEEK composites [21]. In order to investigate the effect of orthotropic electric resistance on the delamination monitoring of cross-ply laminates, several FEM analyses have been also performed [22,23]. Beam type specimens were employed to monitor delamination creations experimentally [24], and plate type specimens of cross-ply laminates were also adopted to monitor the delamination creations experimentally [25]. For the plate type specimens, estimated locations of delamination cracks were discrete levels instead of continuous coordinates to simplify the inverse problems.

In the present study, two types of laminates of different stacking sequences are adopted: cross-ply laminates and quasi-isotropic laminates. An embedded delamination crack is created in a plate type specimen on which multiple electrodes are mounted. Electric resistance

* Corresponding author. Tel.: +81-3-5734-3178; fax: +81-3-5734-3178.

E-mail address: atodorok@ginza.mes.titech.ac.jp (A. Todoroki).

0266-3538/02/$ - see front matter
PII: S0266-3538(02)00053-2

changes of all of the segments between the electrodes are measured with a conventional strain gage amplifier. Using response surfaces, actual location and size of a delamination crack is estimated as continuous values. Applicability of the method for the estimation of continuous values of location and size of a delamination crack is experimentally investigated in detail.

2. Principle of electric resistance change method for delamination monitoring

Graphite fiber has a high electric conductivity, and the epoxy matrix is insulation resistance. For ideal graphite/plastics composites, electric conductance in fiber direction is very high. The ideal conductance can be easily calculated by multiplying fiber volume fraction to electric conductance of graphite fiber. On the other hand, the electric conductance of transverse direction vanishes for an ideal condition.

Practical graphite fiber in a unidirectional ply is serpentine as shown in Fig. 1(a). The curved graphite fiber contacts with each other, and that makes a large graphite-fiber network in a ply. The contact-network brings non-zero electric conductance even in the transverse direction. In the same way, the fiber-network produces non-zero electric conductance in the thickness direction in a ply. The electric conductance in the transverse direction is much lower than the electric conductance of the fiber orientation. Abry et al. [11] and authors [26] have revealed experimentally that the electric conductance ratio of the transverse direction (σ_{90}) to the fiber direction (σ_0) is $\sigma_{90}/\sigma_0 = 3.7\times10^{-2}$, and the electric conductivity ratio of the thickness direction (σ_t) to the fiber direction is approximately $\sigma_t/\sigma_0 = 3.8\times10^{-3}$ for the laminates of the fiber volume fraction of 0.62 ($\sigma_0 = 5500$ S/m). The result tells that the graphite/epoxy laminated composites have very strong orthotropic electric conductance.

The electric conductance of the thickness direction (σ_t) is also lower than the electric conductance of transverse direction (σ_{90}). Although the fiber-network structure in the thickness direction is almost similar to the structure of the transverse direction in a ply, through-the-thickness conductance σ_t is smaller than the σ_{90} for normal laminated composites. That is because thin resin rich interlamina exists and the interlamina is electrically insulating. For ideal graphite/epoxy composites, the σ_t vanishes due to the resin rich interlamina. For practical graphite/plastics composites, however, prepreg plies are serpentine the same as fiber in a ply shown in Fig. 1(b). The curve of plies causes fiber contact through plies and causes non-zero electric conductance in the thickness direction even for thick laminated graphite/epoxy composites. The contact between plies causes no-zero electric conductance in the thickness direction. Thus the σ_{90} is usually larger than the σ_t. When a delamination crack grows in the interlamina, the crack breaks the fiber-contact-network between plies. The breakage of the contact network causes increase of the electric resistance of the graphite/epoxy composites. Therefore, delamination crack can be detected by the electric resistance change of graphite/epoxy composite laminates.

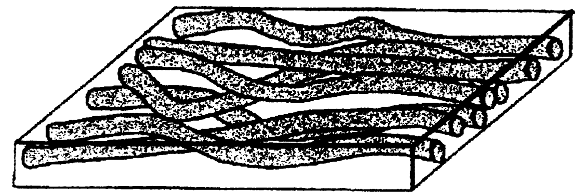

(a)Network structure of fibers in a ply

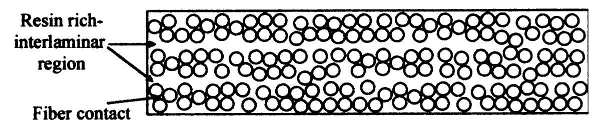

(b)Resin rich-interlamina region and fiber contact

Fig. 1. Schema of practical structure of graphite/epoxy composite.

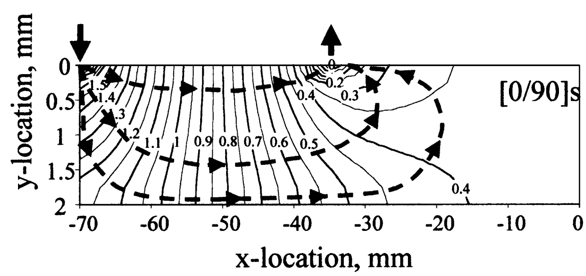

(a) Contour plot of electric voltage of [0/90]s

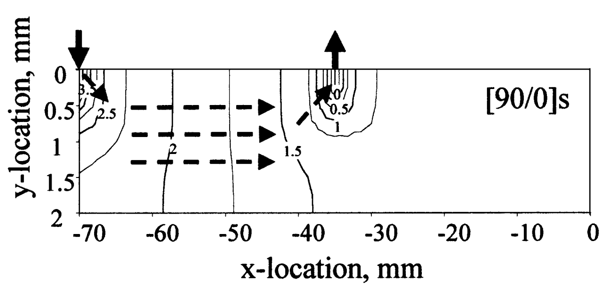

(b) Contour plot of electric voltage of [90/0]s

Fig. 2. Electric voltage contour plot after Ref. [26].

Fig. 2(a) and (b) shows the contour distribution of the electric voltage of FEM results [26] of the [0/90]s laminate and [90/0]s laminate of beam type specimens

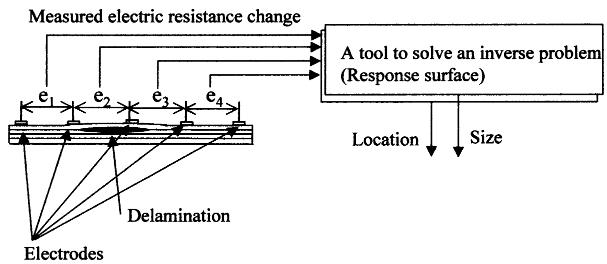

Fig. 3. Schematic representation of delamination identification method using electric resistance change method with response surfaces.

respectively. The ordinate is the distance from the specimen surface where the electric current is charged and abscissa is the location in the longitudinal direction. Electric current 30 mA is charged at the point of $x=-70$ mm and the electric voltage of the point of $x=-35$ mm is fixed to zero. In the case of [0/90]s, where the electric current is charged in the fiber direction in the surface ply, almost half of the electric current flow in the surface ply in the fiber direction, but the rest half of electric current flows in the thickness direction to flow in the 0° ply in the opposite surface when the laminate is thin [26]. The flow in the thickness direction is terminated when a delamination crack exists at the interlamina. This causes electric resistance change owing to the delamination crack for the laminate of [0/90]s. On the other hand, in the case of [90/0]s, where the electric current is charged in the transverse direction in the surface ply, electric current flows in the longitudinal directions, and does not flow in the thickness direction in the middle of the segment between electrodes (from $x=-70$ to -35 mm). A delamination crack is not obstacle for the electric current. Therefore, electric resistance change is not observed for the laminate of [90/0]s. On the basis of the result, electric current should be charged in the fiber direction of the surface ply to detect a delamination crack.

Fig. 3 reveals the schematic representation of the delamination-monitoring system proposed here. Multiple electrodes are mounted on the specimen surface as shown in Fig. 3. All of these electrodes are placed on a single side of a specimen. Usually it is impossible to place electrodes and lead wires outside of the aircraft structures. The location of the electrodes on the single side surface is representative the location of electrodes in the thin aircraft shell type aircraft structures. Electric-resistance change of each segment between electrodes is measured for various cases of location and size of delaminations. Using the measured data, relations between electric resistance change and location and size of delaminations are obtained using response surfaces. Since authors have revealed that the response surfaces are better than artificial neural networks for this inverse problem, the response surface method is employed here [27]. After the calculations of the response surfaces, location and size of a delamination can be estimated with the response surfaces from the measured electric-resistance changes.

3. Response surface for the electric resistance change method

The response surface is a widely adopted tool for quality engineering fields [28]. The response surface methodology comprises curve fitting with regression to obtain approximate responses, design of experiments to obtain minimum variances of the responses and optimizations using the approximated responses.

In the present study, the response surface methodology is adopted as a solver for inverse problems. For the present study, predictions of delamination locations and sizes from measured electric resistance changes are one of the inverse problems. The response surface methodology brings two advantages; the inverse problems can be approximately solved without consideration of modeling, and the approximated response surfaces can be evaluated using powerful statistical tools. For most of the composites, it is very difficult to understand the precise model about electric-resistance change, and other tools like a back-propagation-neural-network have difficulties for evaluations of curve fitness.

For most of the response surfaces, the functions for the approximations are polynomials because of simplicity. For the cases of quadratic polynomials, the response surface is described as follow.

$$y=\beta_0+\sum_{j=1}^{k}\beta_j x_j+\sum_{j=1}^{k}\beta_{jj}x_j^2+\sum_{i=1}^{k-1}\sum_{j=i+1}^{k}\beta_{ij}x_i x_j \qquad (1)$$

where k is the number of variables. In the case of three-electrode type specimens, there are two electric resistance change variables; v_1 and v_2. The response surface for estimations of delamination location (p) is expressed as follow.

$$p=\beta_0+\beta_1 v_1+\beta_2 v_2+\beta_3 v_1^2+\beta_4 v_2+\beta_5 v_1 v_2 \qquad (2)$$

By replacements of

$$y=p,\ x_1=v_1,\ x_2=v_{2,}x_3=v_1^2,\ x_4=v_2^2,\ x_5=v_1 v_2,$$

Eq. (2) becomes a linear regression model.

$$y=\beta_0+\beta_1 x_1+\beta_2 x_2+\beta_3 x_3+\beta_4 x_4+\beta_5 x_5 \qquad (3)$$

In the case that total number of experiments is n, the response surface can be expressed as follows using matrix expression.

$$\mathbf{Y} = \mathbf{X}\boldsymbol{\beta} + \mathbf{e} \tag{4}$$

where

$$\mathbf{Y} = \begin{Bmatrix} y_1 \\ y_2 \\ \vdots \\ y_n \end{Bmatrix} \quad \mathbf{X} = \begin{bmatrix} 1 & x_{11} & x_{12} & \cdots & x_{1k} \\ 1 & x_{21} & x_{22} & \cdots & x_{2k} \\ \vdots & \vdots & \vdots & \ddots & \vdots \\ 1 & x_{n1} & x_{n2} & \cdots & x_{nk} \end{bmatrix}$$

$$\boldsymbol{\beta} = \begin{Bmatrix} \beta_0 \\ \beta_1 \\ \vdots \\ \beta_k \end{Bmatrix} \quad \mathbf{e} = \begin{Bmatrix} \varepsilon_1 \\ \varepsilon_2 \\ \vdots \\ \varepsilon_n \end{Bmatrix}$$

where $\mathbf{e}$ is an error vector.

The unbiased estimator $\mathbf{b}$ of the coefficient vector $\boldsymbol{\beta}$ is obtained using the well known least square error method as follows.

$$\mathbf{b} = \left(\mathbf{X}^T\mathbf{X}\right)^{-1}\mathbf{X}^T\mathbf{Y} \tag{5}$$

The variance-covariance matrix of the $\mathbf{b}$ is obtained as follows.

$$\mathrm{cov}\left(b_i, b_j\right) = C_{ij} = \sigma^2\left(\mathbf{X}^T\mathbf{X}\right)^{-1} \tag{6}$$

where the σ is the error of $\mathbf{Y}$. The estimated value of σ is obtained as follows.

$$\sigma^2 = \frac{SS_E}{n-k-1} \tag{7}$$

SS_E is a square sum of errors, and expressed as follows.

$$SS_E = \mathbf{Y}^T\mathbf{Y} - \mathbf{b}^T\mathbf{X}^T\mathbf{Y} \tag{8}$$

In order to judge the goodness of the approximation of the response surface, the adjusted coefficient of multiple determination R^2_{adj} is used.

$$R^2_{adj} = 1 - \frac{SS_E/(n-k-1)}{S_{yy}/(n-1)} \tag{9}$$

where S_{yy} is the total sum of squares.

$$S_{yy} = \mathbf{Y}^T\mathbf{Y} - \frac{\left(\sum_{i=1}^{n} y_i\right)^2}{n} \tag{10}$$

Each coefficient of the response surface can be tested by using t-statistic. The t-statistic of the coeficient b_j is expressed as follows.

$$t_0 = \frac{b_j}{\sqrt{\sigma^2 C_{jj}}} \tag{11}$$

where the C_{jj} is the element of number jj of variance-covanriance matrix of Eq. (6). When the absolute value of the t-statistics is smaller than the threshold value of t-distribution ($t_{0.025,n\text{-}k\text{-}1}$), the coefficient is eliminated from the response surface as a non-significant coefficient to obtain higher R^2_{adj}.

The response surface (RS) is quite similar to the artificial neural network (ANN) of the famous back propagation training system. The RS has advantages of easy calculations and the availability of the strong statistical tools in compensation for the decrease of fitness compared to the ANN. Our previous paper shows that the RS gives enough approximations for the inverse tool of electric resistance change method for delamination monitoring of graphite/epoxy laminates [27], and the ANN could give larger error for new data that are not used for training. On the other hand, the RS gives better estimations even for the new data. On the basis of the results, the RS is adopted as a tool for solving the inverse problem here.

4. Specimens and experimental procedures

4.1. Specimens

Material used in the present paper is unidirectional graphite/epoxy prepreg. The type of the unidirectional prepreg sheet is TR340M150ST produced by Mitsubishi-Rayon Co. Ltd.. Using the prepreg, cross-ply laminates of $[0_2/90_2]$s and quasi-isotropic laminates of [0/45/−45/90]s were fabricated. The fiber volume fraction is approximately 0.5. Thickness of the laminates is approximately $t = 1$ mm. Cure condition is 130 °C×1.1 MPa×1 h using a hot press. In order to measure electric-resistance changes using a two-probe method, reliable electrodes are indispensable. In order to produce the reliable electrodes, rectangle copper foil of 0.02 mm thickness is mounted on the prepreg laminates, and these electrodes are co-cured with the laminate. From the laminates, rectangular plate type specimens of the length of 200 mm and the width of 105 mm were produced as shown in Fig. 4. The multiple electrodes are mounted on a single surface of the specimen in the present study as previously mentioned.

4.2. Electric circuit

Since electric-resistance change due to a delamination crack creation is very small, the electric-resistance change is measured with the electric-resistance bridge circuit as shown in Fig. 5. As easily recognized, the

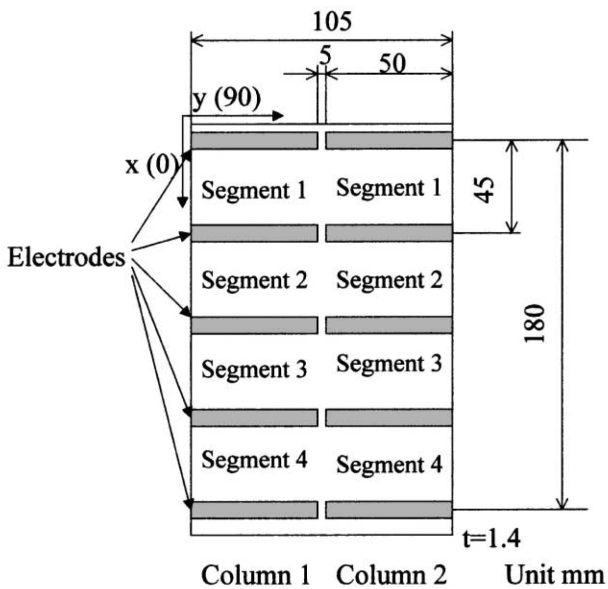

Fig. 4. Specimen configuration.

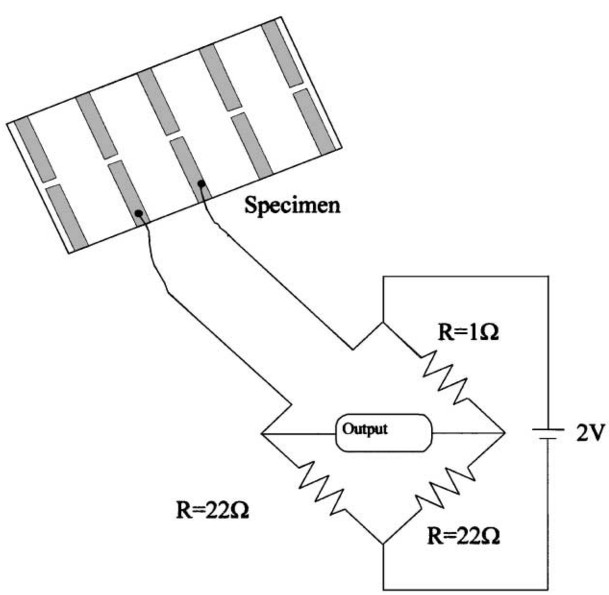

Fig. 5. Electric bridge circuit.

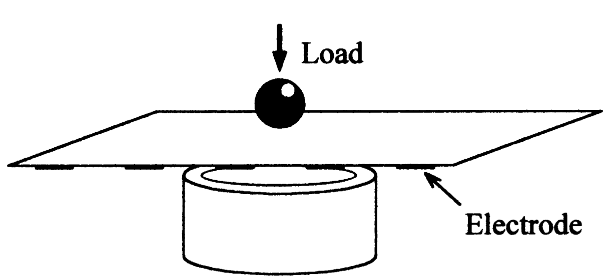

Fig. 6. Indentation procedure of the laminates to create a delamination crack.

bridge circuit is quite similar to that of the conventional strain gages. Therefore, conventional strain-gage amplifiers are adopted for measurements of electric resistance change of the specimens without any changes. That brings about that the output of the instrument is "strain", but it does not mean deformation of the specimens. The output "strain" means electric-resistance change ratio here. The electric-resistance change ratio is expressed using output "strain" data ε as follows.

$$\frac{\Delta R}{R} = k\varepsilon \tag{12}$$

where, ΔR is the electric-resistance change due to a creation of a delamination crack, R is an initial electric resistance, k is a gage factor, and ε is a measured output "strain". Usually the gage factor adopted for the conventional strain-gage amplifier is 2. In order to obtain higher output "strain" data, the electric-resistance change ratio $\Delta R/R$ should be large. Since the electric-resistance change (ΔR) is very small and the measured initial electric resistance (R) of the specimen is approximately 1 Ω , the electric resistances of the bridge circuit are arranged from the normal circuit for conventional strain gages. By trial and error, electric resistance of 22 Ω is selected as another resistance R in this bridge circuit. Since the measured output is ε, ε is called as electric-resistance change ($v = \Delta R/R/k$) in the present study though it still includes the effect of the gage factor.

4.3. Experimental procedures

In order to create a delamination crack in each plate-type specimen, an indentation test is employed here. As shown in Fig. 6, an indentation type jig and cylindrical support is adopted here. By changing the diameter of the cylindrical support jig from 10 to 50 mm, several sizes of delamination were created in the plate type specimen. Since the method employs a two-probe method, the electrodes are avoided for the indentation tests to prevent electric resistance change at the electrodes. This could be improved when a four-probe method is employed. The indentation point is loaded from the opposite side surface where the electrodes are mounted. This is to simulate the placements of electrodes inside of the structures and the impact load that creates a delamination comes from the outside. Since the specimen is a thin laminate, the loading creates a large delamination crack in the 0–90° interface near the electrodes.

After creating a delamination crack, electric-resistance changes of all segments between electrodes were measured using a conventional strain amplifier. Delamination location and size were measured using an ultrasonic C-scan image. The delamination location is decided at the center point of the delamination crack from the specimen end. Since the location in the plate type specimen has two directions, two directions of x-direction (0°-direction) and y-direction (90°-direction) are decided for the identification of the delamination location. The delamination size corresponds to the maximum diameter of the delamination crack.

5. Results and discussion

5.1. Delamination and electric resistance changes

Typical examples of the C-scan images of the created delamination cracks of cross-ply laminates and quasi-isotropic laminates are shown in Figs. 7 and 8. These delamination cracks include the matrix cracks, and these are completely embedded in the laminates like practical delamination cracks. From the visual inspection, no fiber breakage is observed. As shown in Figs. 7(b) and 8(b), a larger delamination crack is created near the surface where the electrodes are mounted. This is because the indentation loading is performed from the opposite surface where the electrodes are mounted, as explained by Suemasu and Majima [29]. Since the laminates are thin, location of the delamination along the thickness direction is almost the same for all specimens. In the present study, therefore, only the location of x-direction and y-direction of the delamination is discussed.

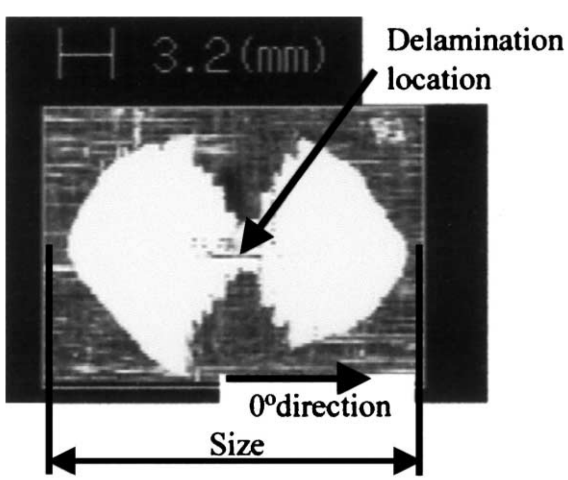

Fig. 7. Delamination crack of cross-ply laminate by ultrasonic C-scan image.

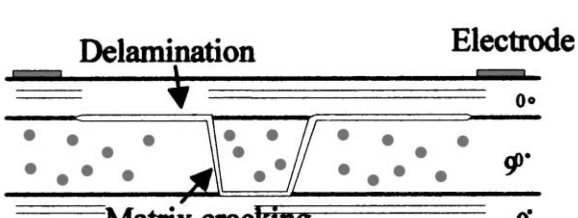

Fig. 8. Schematic image of cross section of delamination.

Typical experimental results obtained after delamination creations are shown in Figs. 9 and 10. The measured electric resistance changes of all the segments between electrodes of the cross-ply laminate is shown in Fig. 9(a) and (b). The measured electric resistance changes of all the segments between electrodes of the quasi-isotropic laminate is shown in Fig. 10(a) and (b). Figs. 9(a) and 10(a) show the results in the case of a delamination of approximately 20 mm in the first column ($y = 68$ mm) and in the second segment ($x = 22$ mm). Figs. 9 (b) and 10 (b) show the results in the case of a delamination of approximately 20 mm between the first and second columns and in the second segment. For all these figures, the ordinate is the measured electric resistance ratio of each segment and the abscissa is the segment number. The solid lines show the results of the first column and the broken lines show the results of the second column.

For both laminates, only the electric resistances of the first column change and the electric resistances in the second column do not change when the delamination is located in the first column (the solid line cases). On the other hand, when the delamination is located between the first and second columns [see Figs. 9(b) and 10(b)], electric resistance changes in the two columns are

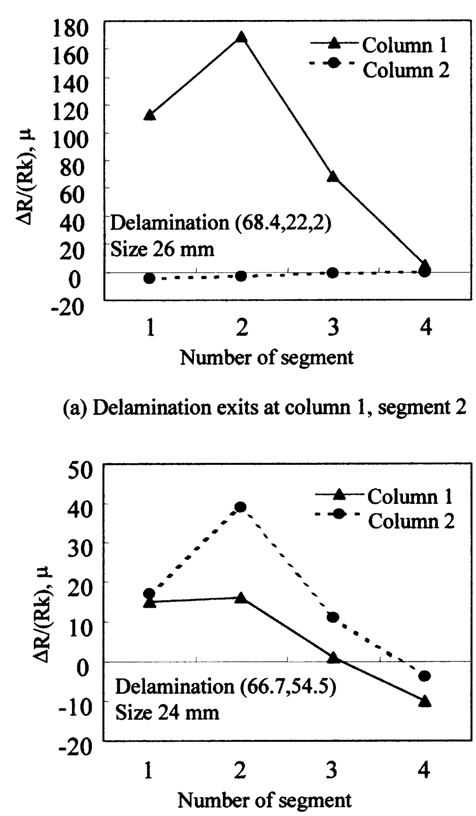

(a) Delamination exits at column 1, segment 2

(b) Delamination exits at the middle of the both columns, segment 2

Fig. 9. Typical measured electric resistance change ratio of cross-ply laminate.

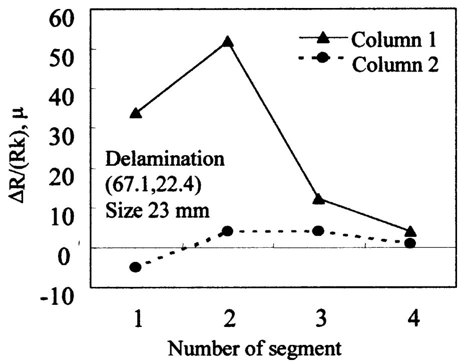

(a) Delamination exits at column 1, segment 2

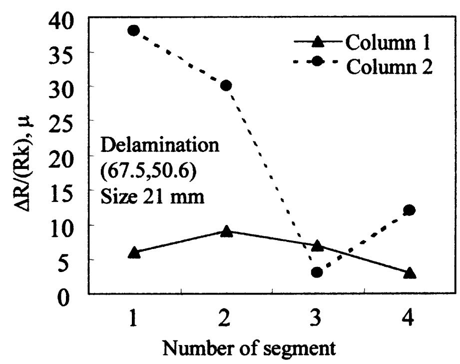

(b) Delamination exits at the middle of the both columns, segment 2

Fig. 10. Typical measured electric resistance change ratio of quasi-isotropic laminate.

measured. Although the delamination exists in the second segment in all cases, electric resistance changes in the first and third segments are measured. Moreover, in Fig. 10(b), the electric resistance change of the first segment is larger than the second segment.

The electric resistance changes in the adjacent segments where delamination does not exist are due to the strong orthotropic electric conductance of graphite/epoxy laminates. As shown in Fig. 2(a), electric current flows even in the adjacent segments. These circular electric currents cause electric resistance changes in the adjacent segments.

It causes the identification of delamination difficult that a maximum in the electric resistance change does not always imply the existence of a delamination in the segment. Similar electric resistance changes are observed in the FEM analyses of beam type specimens [26]. From this complexity, it is easily recognized that the estimation of the location of a delamination by a continuous value is a quite difficult problem.

The electric resistance change values of the cross-ply laminates are larger than those of the quasi-isotropic laminates by the factor of three. This is owing to the delamination location in the thickness direction. For the quasi-isotropic laminates, the delamination exists at the interface between the 45° ply and −45° ply that locates far from the surface.

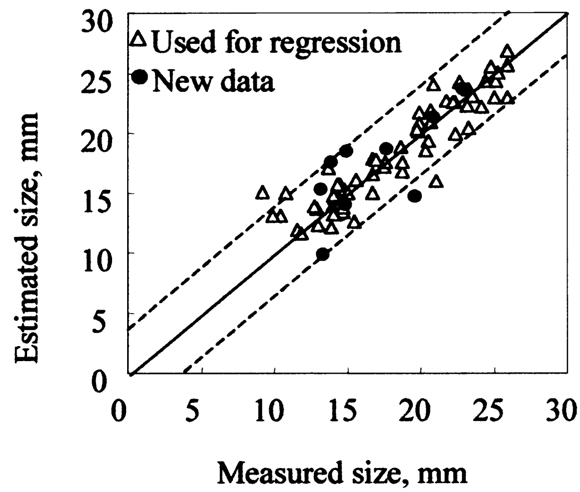

Fig. 11. Estimation results of delamination size for cross-ply laminate (open triangle: estimated results of the data used for regression; closed circle: estimated results of the data not used for the regression).

5.2. Identification of the delamination size

Using the measured electric resistance data sets (number of the data sets is 64), response surfaces to estimate the delamination size from measured electric resistance changes are obtained. For the cross-ply laminates, the adjusted coefficient of multiple determination R^2_{adj} is 0.77, and the R^2_{adj} for the quasi-isotropic laminates is 0.86. Both response surfaces give excellent approximations.

Estimations for the data used for the regressions and for the new data that are not used for the regressions are performed to evaluate the efficiency of the estimations of the response surfaces. For the cross-ply laminates, the number of the new data is 9, and the number of the new data for the quasi-isotropic laminates is 6. Both of the estimation results are shown in Figs. 11 and 12 respectively. For the figures, the ordinate is the estimated delamination size with the response surface, and the abscissa is the measured delamination size with the ultrasonic C-san image. Symbols plotted on the diagonal line represent the good estimations. The triangular symbols represent the data used for regression and the filled circle symbols represent the new data that are not used for regression. Both figures show that the estimates give good predictions of the measured delamination size. Moreover, we can conclude that a delamination of larger than 10 mm can be detected with the method.

Since the measurement of delamination size with the ultrasonic C-scan image has an error of 3 mm approximately, practical estimation performance is defined that estimation error of 3 mm is tolerance for practical use. In each figure, dotted lines show the error bands of 3

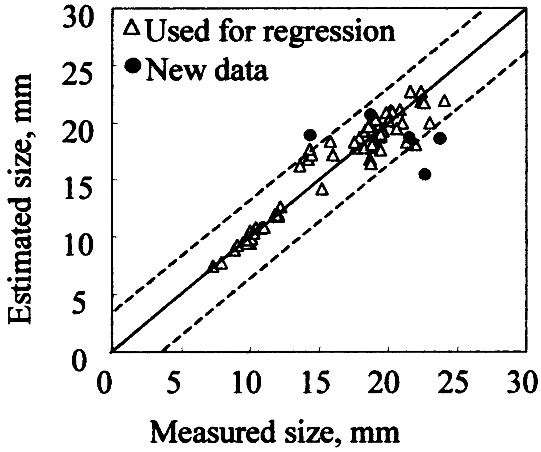

Fig. 12. Estimation results of delamination size for quasi-isotropic laminate (open triangle: estimated results of the data used for regression; closed circle: estimated results of the data not used for the regression).

mm. As shown in these figures, most of the data are located inside of the error bands. For the cross-ply laminates, the practical performance of estimations including the new data is 95.9%, and for the quasi-isotropic laminates, the practical performance of estimations including the new data is 95.7%. From these results, we can conclude that the estimations of delamination size with the response surfaces are excellent.

5.3. Identification of delamination location

In order to estimate the location of delamination crack in a plate, we need two response surfaces; x-direction and y-direction. For the cross-ply laminates, the R^2_{adj} of the response surface of x-direction is 0.80 and the R^2_{adj} of y-direction is 0.73. For the quasi-isotropic laminates, the R^2_{adj} of the response surface of x-direction is 0.63 and the R^2_{adj} of y-direction is 0.70. The approximations for the location of delamination is not good compared to the estimations of the delamination size. Especially, for the isotropic laminates, the R^2_{adj} is nearly 0.6. That means the approximations could be poor.

For each laminates, substituting the measured electric resistance changes into the response surfaces of x-direction and y-direction, estimations of the delamination location are performed, and the estimations for the new data are also conducted. The estimation results are shown in Figs. 13 and 14 respectively. The ordinate is the estimated location of delamination and the abscissa is the measured delamination location. The open triangular symbols show the results of the estimations of the data used for the regression, and the solid circle symbols show the estimations of the new data.

As shown in Fig. 13, the estimation results of the cross-ply laminates present relatively a good agreement with the measured results. On the other hand, the estimations of the quasi-isotropic laminates give large

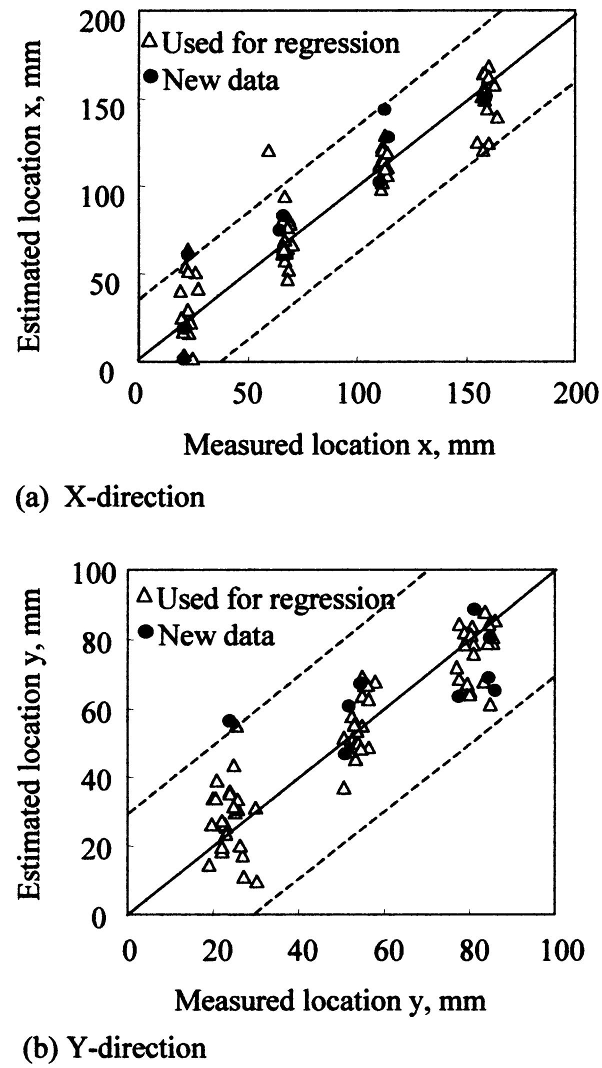

Fig. 13. Estimation results of delamination location for cross-ply laminate (open triangle: estimated results of the data used for regression; closed circle: estimated results of the data not used for the regression).

errors as shown in Fig. 14. In order to evaluate the practical performances, we have to decide the tolerance error band of delamination location. In the present study, the error band is set to 30 mm, that is a slightly smaller value than the spacing of the electrode segment (50×45 mm). The dotted lines show the error band in the figures. The practical performance of the cross-ply laminates is 95.9% (x-direction) and 98.6% (y-direction). For the quasi-isotropic laminates, the practical performance is 87.1% (x-direction) and 97.1% (y-direction). The estimations for the cross-ply laminates are excellent. For the quasi-isotropic laminates, on the other hand, practical performance of the estimations marginal, and it requires improvement.

The small electric resistance changes of the quasi-isotropic laminates cause the large error of the estimations of the location of the delamination. One reason of

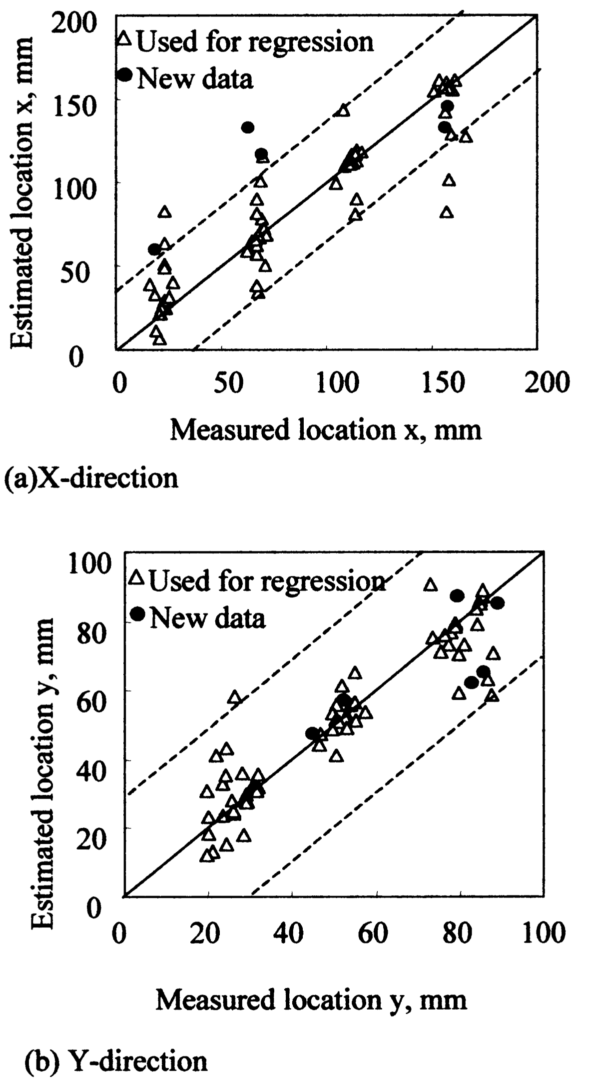

Fig. 14. Estimation results of delamination location for quasi-isotropic laminate (open triangle: estimated results of the data used for regression; closed circle: estimated results of the data not used for the regression).

the small change is the delamination locates far from the surface. This could be improved by charging higher electric current. Another reason is the experimental error due to the limited reliability of co-cured electrodes. This is improved by using the four-probe method for the measurements of electric resistance change.

6. Conclusions

In the present study, identifications of the location and size of a delamination crack of laminated graphite/epoxy plates are performed using the electric resistance change method with response surfaces. Cross-ply laminates and quasi-isotropic laminates are prepared for experiments. The results obtained are as follows.

1. Delamination size identifications with response surfaces can be successfully performed for both types of laminates.
2. For the cross-ply laminates, the identifications of delamination location can be successfully performed.
3. For the quasi-isotropic laminates, identifications of delamination location give marginal estimations, and the method must be improved for practical applications.

References

[1] Moriya K, Endo T. A study on flaw detection method for cfrp composite laminates (1st report) the measurement of crack extension in cfrp composites by electrical potential method. Aeronautical and Space Science Japan 1988;36(410):139–146 [in Japanese].
[2] Schulte K, Baron Ch. Load and failure analyses of CFRP laminates by means of electrical resistively measurements. Composites Science and Technology 1989;36:63–76.
[3] Muto N, Yanagida H, Miyayama M, Nakatsuji T, Sugita M, Ohtsuka Y. Foreseeing of fracture in CFGFRP composites by measuring electric resistance. J Japan Society Composites Materials 1992;18(4):144–50 [in Japanese].
[4] Fischer Chr, Arendts FJ. Electrical crack length measurement and the temperature dependence of the mode I fracture toughness of carbon fibre reinforced plastics. Composites Science and Technology 1993;46:319–23.
[5] Chen PW, Chung DDL. Carbon fiber reinforced concrete for smart structures capable of non-destructive flaw detection. Smart Mater Struct 1993;2:22–30.
[6] Kaddoour AS, Al-Salehi FA, Al-Hassani STS. Electrical resistance measurement technique for detecting failure in CFRP materials at high strain rate. Composites Science and Technology 1994;51:377–85.
[7] Wolfiger C, Drechsier K. Damage detection in composite materials by monitoring electrical impedance. In: Proc. of the Int. Symp. on Advanced Materials for Lightweight Structures, ESTEC, Noordwijk (ESA-WPP-070); 1994. p. 677–782.
[8] Chen PW, Chung DDL. Carbon-fiber-reinforced concrete as intrinsically smart concrete for damage assessment during dynamic loading. J Am Ceram Soc 1995;78(3):816–8.
[9] Wang X, Chung DDL. Sensing delamination in a carbon fiber polymer-matrix composite during fatigue by electrical resistance measurement. Polymer Composites 1997;18(6):692–700.
[10] Irving PE, Thiagarajan C. Fatigue damage characterization in carbon fibre composite materials using an electric potential technique. Smart Materials and Structures 1998;7:456–66.
[11] Abry JC, Bochard S, Chateauminois A, Salvia M, Giraud G. In situ detection of damage in CFRP laminates by electric resistance measurements. Composites Science and Technology 1999;59:925–35.
[12] Seo DC, Lee JJ. Damage detection of CFRp laminates using electrical resistance measurement and neural network. Composites Structures 1999;47:525–30.
[13] Abry JC, Choi YK, Chateuminois A, Dalloz B, Giraud G. In-situ monitoring of damage in CFRP laminates by means of AC and DC measurements. Composites Science and Technology 2001;61: 855–64.

[14] Weber I, Schwartz P. Monitoring bending fatigue in carbon-fiber/epoxy composite strands: a comparison between mechanical and resistance techniques. Composites Science and Technology 2001;61:849–53.

[15] Muto N, Arai Y, Shin SG, Matsubara H, Yanagaida H, Sugita M, Nakatsuji T. Hybrid composites with self-diagnosing function for preventing fatal fracture. Composites Science and Technology 2001;61:875–83.

[16] Kupke M, Schulte K, Schuler R. Non-destructive testing of FRP by DC and AC electrical method. Composites Science and Technology 2001;61:837–47.

[17] Schueler R, Joshi SP, Schulte K. Damage detection in CFRP by electrical conductance mapping. Composites Science and Technology 2001;61:921–30.

[18] Kubo S, Kuchinishi M, Sakagami T, Ioka S. Identification of delamination in layered composite materials by the electric potential CT method. Applied electromagnetics and mechanics. In: Takagi T, Uesaka M, editor. Proc. of the 10th Int. Symp. on Applied Electromagnetics and Mechanics, Japan Soc. Applied Electromagnetics and Mechanics. 2001. p. 641–642.

[19] Todoroki A, Matsuura K, Kobayashi H. Application of electric potential method to smart composite structures for detecting delamination. JSME International J, Series A 1995;38(4):524–30.

[20] Todoroki A, Kobayashi H, Matsuura K. Application of electrical potential method as delamination sensor for smart structures of graphite/epoxy. In: Inoue K, Shen SIY, Taya M, editors. US-Japan Workshop on Smart Materials and Structures. TMS: University of Washington; 1997. p. 47–54.

[21] Todoroki A. Delamination detection by electric resistance change for graphite/PEEK composites. In: Proceedings of the 5th Japan International SAMPE Symposium; 1997. p. 899–904.

[22] Todoroki A, Suzuki H, Kobayashi H, Nakamura H, Shimamura Y. Evaluation of orthotropic electrical resistance for delamination detection of CFRP by electrical potential method. Transactions of the Japan Society of Mechanical Engineers Series A 1998;64(622):1654–1659 [in Japanese].

[23] Todoroki A, Suzuki H. Health monitoring of internal delamination cracks for graphite/epoxy composites by electric potential method. Applied Mechanics and Engineering 2000;5(1):283–94.

[24] Todoroki A, Tanaka Y, Shimamura Y. Response surface for delamination monitoring of graphite/epoxy composite using electric resistance change, structural health monitoring 2000 [edited by F.K. Chang]. Technomic 1999:308–16

[25] Todoroki A, Tanaka Y, Shimamura Y. Electric resistance change method for identification of embedded delamination of CFRP plates. Materials Science Research International, Special Technical Publication-2, JSMS; 2001. p. 139–145.

[26] Todoroki A, Tanaka M, Shimamura Y. Measurement of orthotropic electric conductance of CFRP laminates and analysis of the effect on delamination monitoring with electric resistance change method. Composites Science and Technology 2002;62(5):619–28.

[27] Todoroki A. Effect of number of electrodes and diagnostic tool for delamination monitoring of graphite/epoxy laminates using electric resistance change. Composites Science and Technology 2001;61(13):1871–80.

[28] Myers R, Montgomery DC. Response surface methodology process and product optimization using designed experiments. New York: Wiley Inter-science Publication; 1995.

[29] Suemasu H, Majima O. Multiple delaminations and their severity in nonlinear circular plate subjected to transverse loadings. J Composite Materials 1998;32(2):123–40.